Available online at www.sciencedirect.com
SCIENCE DIRECT
Bioorganic & Medicinal Chemistry 14 (2006) 1729–1736
Bioorganic & Medicinal Chemistry

Enantiomeric *N*-methyl-4-piperidyl benzilates as muscarinic receptor ligands: Radioligand binding studies and docking studies to models of the three muscarinic receptors M1, M2 and M3

Jana Selent,[a] Wolfgang Brandt,[b,*] Dirk Pamperin[c] and Berthold Göber[a]

[a]*Department of Chemistry, Humboldt-University of Berlin, Brook-Taylor-Str. 2, D-12489 Berlin, Germany*
[b]*Department of Bioorganic Chemistry of the Leibniz Institute of Plant Biochemistry, Weinberg 3, D-06120 Halle/Saale, Germany*
[c]*Apogepha Arzneimittel GmbH, Kyffhäuserstr. 27, D-01309 Dresden, Germany*

Received 19 July 2005; revised 7 October 2005; accepted 13 October 2005
Available online 14 November 2005

Abstract—Benzilic ester derivatives with a basic moiety like *N*-methyl-4-piperidyl benzilates are potential drugs for the treatment of urinary incontinence, duodenal and gastric ulcers and Parkinson's disease. The effect of structural variations of chiral *N*-methyl-4-piperidyl benzilates was investigated using radioligand binding studies on muscarinic receptors (M_1–M_3). The results of the binding studies demonstrate that the absolute configuration and the aromatic substituent of benzilates have an influence on muscarinic affinity and selectivity. In this regard, (*S*)-configuration of benzilates and hydrophilic aromatic substituents seems to enhance muscarinic affinity. A model of the receptor ligand complex for *N*-methyl-4-piperidyl benzilates was obtained by molecular modelling. Both the affinity of enantiomeric benzilic esters and the subtype selectivity for muscarinic receptors are comprehensively explained by this model.

1. Introduction

Muscarinic receptors are members of the seven transmembrane G protein coupled receptor (GPCR). They are well known as mediators for pharmacological responses in a wide range of clinical important indications. The different muscarinic receptor subtypes (M1–M5) have been extensively investigated.[1–3] In order to control the diverse response of muscarinic receptor subtypes, there has been a strong effort to develop selective ligands. Atropine, a natural compound and a classical muscarinic receptor antagonist, fails to discriminate among muscarinic receptor subtypes. Low subtype selectivity of compounds restricts their pharmaceutical application because of anticholinergic side effects. Selective antagonists are known like pirenzepine a synthetic drug with a high affinity for the M1 receptor and use for gastric ulcers.[4] Substances, which feature M3 selectivity, are applied for urinary incontinence.[5–8]

Although there is extensive knowledge about muscarinic receptor subtypes, the structural design of selective compounds is problematic as receptor subtypes possess more than 70% identity. Particularly, the transmembrane domain is known to be a highly conserved region within the muscarinic subtypes. Most small sized muscarinic antagonists bind into the same transmembrane binding pocket, that is, ligands interact with similar or even identical amino acids for different subtypes. Larger sized ligands are assumed to interact with extracellular loops rather than with transmembrane helices.[9] This could provide a higher selectivity because larger deviations of sequence homology are found in the extracellular region. However, high flexibility of the extracellular region makes it difficult to determine the structural requirements for a selective compound.

Racemic *N*-methyl-4-piperidyl benzilates have been thoroughly investigated with respect to their anticholinergic effect.[10,11] As the stereochemistry of benzilates is thought to have an influence upon receptor

Abbreviations: 4-DAMP, 4-diphenylacetoxy-*N*-methylpiperidine methiodide; E, extracelluar loop; E_L, energy of the isolated ligand; E_R, energy of the empty receptor; E_{RL}, energy of the receptor ligand complex; GPCR, G protein coupled receptor; H, helix; I, intracelluar loop; IE, interaction energy; M1–M5, muscarinic receptor subtypes; NMS, *N*-methylscopolamine.

Keywords: Chiral benzilic acid derivatives; Muscarinic antagonists; Muscarinic receptors (M1, M2, M3); Molecular modelling.

* Corresponding author. Tel.: +49 345 55821360; fax: +49 345 55821309; e-mail: wbrandt@ipb-halle.de

0968-0896/$ - see front matter © 2005 Elsevier Ltd. All rights reserved.
doi:10.1016/j.bmc.2005.10.030

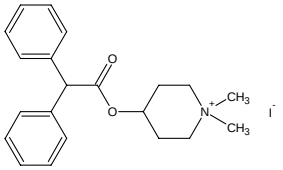

Figure 1. Structure of M3 selective 4-DAMP.

affinity and selectivity, the objective of this thesis was to determine the diverse affinities of enantiomeric substituted *N*-methyl-4-piperidyl benzilates in radioligand binding studies to M1, M2 and M3. The enantiomers can be obtained either by enantioselective synthesis or separation via distomeric salt formation, preferential crystallization and chromatographic methods.[12]

The essential pharmacophoric structures of *N*-methyl-4-piperidyl benzilates and related antimuscarinics contain two large hydrophobic groups in α-position to an ester function which is connected to a tertiary or quaternary nitrogen over two or three carbon atoms. Additionally, a particular conformation seems to have an effect on the magnitude of the affinity, whereas conformation B (Fig. 6) is preferred by the muscarinic receptor.[13] Furthermore, the M3 selectivity of 4-DAMP has to be ascribed to a certain conformation because obviously 4-DAMP does not possess particular structural elements which impart selectivity (Fig. 1).[14]

In an attempt to disclose the structural elements of benzilic compounds which impart a magnitude of affinity and/or selectivity, both aromatic substitution with varying electronical properties and the absolute configuration of the central asymmetrical carbon atom were modified (Table 1). The diverse affinities of the substituents with opposite properties (e.g., *tert*-butyl and trifluoromethoxy) may presumably contribute new aspects of the binding site topography.

The binding site of muscarinic agonists and antagonists has been the subject of a multitude of publications, in which the importance of certain amino acids of the receptor protein was determined by intensive mutagenesis studies. Asp105, Tyr106, Tyr381, Asn382, Tyr404, Cys407 and Tyr408 are particularly important residues for the antagonist *N*-methylscopolamine (NMS). The phenyl ring of NMS is expected to be close to Asn110.[15] Mutation of Asn382 decreased the affinity by 1000- to 3000-fold, whereas 100-fold reduction occurred by mutation of Asp105, Tyr106 and Trp157. Asn110, Tyr404 show smaller effects (10- to 20-fold reduction).[16] The agonist acetylcholine binds in a similar manner as NMS. Formation of a salt bridge from the carboxylic function of Asp105 to the ammonium group is essential for the acetylcholine binding. This salt bridge has also been discussed for antagonistic effects.[17]

2. Results and discussion

2.1. Radioligand binding studies

The binding properties of eight enantiomeric benzilates (Table 1) were investigated for three human muscarinic

Table 1. Enantiomeric target structures of *N*-methyl-4-piperidyl benzilate

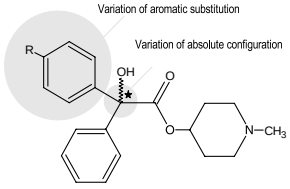

Absolute configuration		Aromatic substitution *R*
R	*S*	
1	**2**	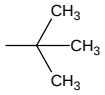
3	**4**	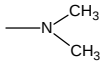
5	**6**	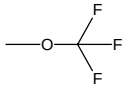
7	**8**	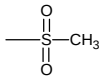

receptor subtypes (M1, M2 and M3) expressed in stably transfected CHO cells (Table 2). [^{3}H]-*N*-methylscopolamine was used as radioligand. With the exception of (*S*)-*N*-methyl-4-piperidyl 4-trifluormethoxybenzilate (**6**), all compounds showed equal or highest affinity for the M1-receptor. The affinity for the M3-receptor was higher than that for the M2-receptor (M1 > M3 > M2). The (*S*)-enantiomer of 4-dimethylaminobenzilate (**4**) is eminent with 50-fold M1/M2 and 33-fold M1/M3. Consequently, (*S*)-*N*-methyl-4-piperidyl 4-dimethylaminobenzilate (**4**) is a M1 selective compound and comparable to pirenzepine which is applied for the treatment of gastric ulcers. Interestingly, the (*S*)-configuration of all enantiomeric compounds showed higher affinity for all muscarinic subtypes, whereas the proportion M1 > M3 is shifted to M1 ≫ M3. Although M1 affinity is always dominant, (*R*)-configuration seems to enhance the M3 affinity (M1 ≫ M3 shifted to M1 ⩾ M3). Thus M1 selectivity of (*S*)-configured 4-dimethylaminobenzilate (M1/M3: 33-fold) is completely abolished by conversion of the asymmetric carbon atom to (*R*)-configuration (M1/M3: 4-fold). Identical potency at M1 and M3 is found for 4-*tert*-butylbenzilate (**1**). Hence, (*R*)-configured benzilates may be considered as pharmaceutical leads concerning M3 selective compounds, that is, a drug against incontinence.

The eudismic ratio, which is the potency of eutomer (*S*) relative to that of the distomer (*R*), depends on the type of aromatic substituents of the benzilic structure (Fig. 2). Interestingly, the difference in affinity for the corresponding (*R*)- and (*S*)-enantiomers is low for hydrophobic substituents (*tert*-butyl), while polar substituted benzilates (dimethylamino-, trifluormethoxy- and methylsulfonyl-) cause a much higher affinity difference. This implies an additional polar interaction

Table 2. Binding constants pK_i of enantiomeric benzilates, standard errors and binding ratios of M1/M2, M1/M3 and M3/M2

Substitution R		Binding constant pK_i			Binding ratio		
		pK_i (M1)	pK_i (M2)	pK_i (M3)	M1/M2 = K_i (M2)/K_i (M1)	M1/M3 = K_i (M3)/K_i (M1)	M3/M2 = K_i (M2)/K_i (M3)
(*R*) 4-*tert*-C_4H_9–	(**1**)	7.52 ± 0.05	6.69 ± 0.09	7.52 ± 0.06	6.8	1	6.8
(*S*) 4-*tert*-C_4H_9–	(**2**)	8.29 ± 0.04	7.48 ± 0.07	7.84 ± 0.05	6.5	2.8	2.3
(*R*) 4-$(CH_3)_2N$–	(**3**)	7.34 ± 0.08	6.73 ± 0.03	7.08 ± 0.09	4.1	1.8	2.2
(*S*) 4-$(CH_3)_2N$–	(**4**)	8.98 ± 0.10	7.28 ± 0.07	7.46 ± 0.02	50.1	33.1	1.5
(*R*) 4-F_3CO–	(**5**)	7.39 ± 0.10	6.84 ± 0.08	7.08 ± 0.09	3.5	2.0	1.7
(*S*) 4-F_3CO–	(**6**)	8.91 ± 0.06	8.61 ± 0.04	8.40 ± 0.06	2.0	3.2	0.6
(*R*) 4-CH_3SO_2–	(**7**)	6.58 ± 0.16	5.8 ± 0.04	6.39 ± 0.02	6.0	1.5	3.9
(*S*) 4-CH_3SO_2–	(**8**)	8.37 ± 0.08	7.15 ± 0.17	7.77 ± 0.04	16.6	4.0	4.2
Reference							
Pirenzepine[a] (M1 selective)		8.1	6.3	6.7	63	25	2.5
4-DAMP[b] (M3 selective)		8.8	8.1	9.1	5.0	0.5	10

a

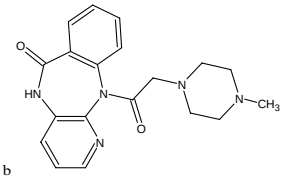

b

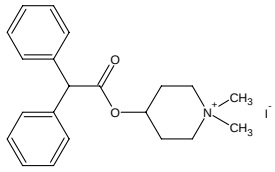

with the substituted ring of (*S*)-configured benzilates in the protein binding pocket. These additional interactions are presumably responsible for the observed higher affinities of (*S*)-enantiomers for all subtypes compared to (*R*)-enantiomers (e.g., methylsulfonyl *S*/*R*: 22- to 62-fold at M1, M2 and M3), while the binding difference for hydrophobic analogues almost vanished because of missing extra attractive interactions (*tert*-butyl *R*/*S*: 2- to 6-fold at M1, M2 and M3). With respect to the binding site topography of the receptor protein, it is further implied that a concentration of polar amino acids is located in a certain transmembrane region to interact with the substituted phenyl ring of (*S*)-configured benzilates.

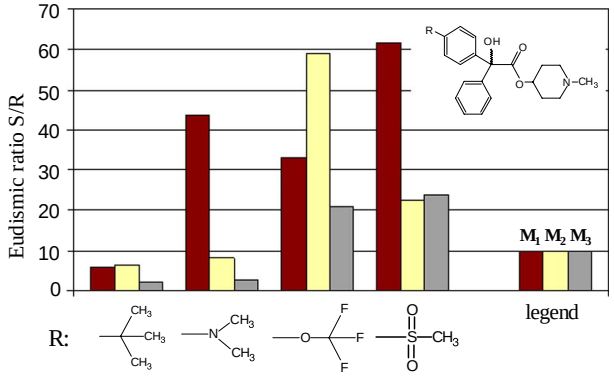

Figure 2. Eudismic ratio of enantiomeric benzilates on muscarinic receptor subtypes M1/M2/M3.

Furthermore, the alcoholic component of the benzilic ester has an influence upon muscarinic selectivity. While *N*-methyl-4-piperidyl benzilates exhibit higher affinity towards M1 and M3 (M1 > M3), (*R*)-quinuclidinyl benzilates are characterized by higher affinity at M1 and M2.[18] Consequently, *N*-methyl-4-piperidol as the alcoholic component intensifies M3 affinity, whereas (*R*)-quinuclidinol enhances affinity for M2 (Fig. 3).

2.2. Molecular modelling

Based on the X-ray structure of bovine rhodopsin muscarinic receptors M1, M2 and M3 have been modelled. Subsequently, the resulting receptor models were used for docking studies. Radioligand binding studies revealed that substituted *N*-methyl-4-piperidyl benzilates competitively displace the radioligand [^{3}H]NMS. Accordingly, the binding sites of both ligands should be located in an overlapping transmembrane region. Therefore, a docking region of 15 Å surrounding the amino acid Asp105, which is essential for binding, was specified for the docking experiments of enantiomeric benzilates. The ligands were introduced in a protonated form (protonated nitrogen in the piperidyl ring).

The calculated docking arrangements of all ligands and receptor subtypes show a fundamental analogy of receptor ligand interactions. The involved amino acids of the suggested transmembrane binding pocket are listed in Table 3. Non-conserved amino acids within the receptor subtypes (M1–M3), which interact directly with the ligand and presumably play an important role for

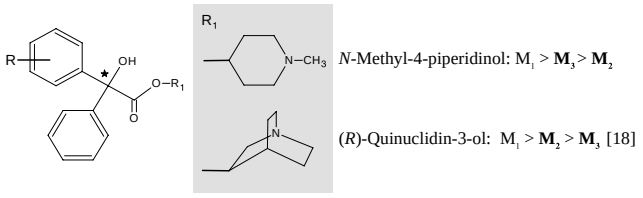

Figure 3. Diverse affinities on M1/M2/M3 receptors in dependency of the alcoholic component R_1.

different affinities for subtypes, are tagged in Table 3. The location of these binding amino acids is also depicted in the snake-like presentation in Figure 4. The relevant amino acids, which are found in the binding pocket of our model, basically correspond to the one described by Hulme et al. for NMS.[15–17]

The following binding interactions are identical for all benzilic esters at receptor subtypes M1, M2 and M3 (Fig. 5, **A**):

- Formation of a salt bridge between the protonated nitrogen of the piperidyl ring and Asp105.
- Side chains of Tyr404 and Tyr408 stabilize the arrangement of the piperidyl ring through hydrophobic interactions, in particular between Tyr404 and *N*-methyl group of the piperidyl ring.
- Additionally, intermolecular interactions of Asp105 and Tyr404 result in an appropriate positioning of the carboxylic function of Asp104 which is essential for salt bridge formation.

2.2.1. Affinity distinctions of enantiomeric benzilates ((*S*)-enantiomers > (*R*)-enantiomers). The resulting model gives an explanation for the tendency of (*S*)-configured benzilates to bind with higher potency into the binding pocket. According to the proposed model (Fig. 5, **A**) the substituted phenyl ring of (*S*)-configured benzilates interacts preferably with the *S*-site. Indeed, there are hydrophilic amino acids in the *S*-site such as Asn110 and Thr202 which are capable of forming hydrogen bridges (methlysulfonyl-, dimethylamino-) or attractive polar interactions (trifluormethoxy-) substituted ligands.

Table 3. Relevant amino acids of the binding pocket of M1-, M2- and M3-receptors

M_1	M_2	M_3	Region[a]	Comment
Asp105	Asp103	Asp148	H3	Salt bridge
Tyr106	Tyr104	Tyr149	H3	*S*-site
Ser109	Ser107	Ser152	H3	*S*-site
Asn110	Asn108	Asn153	H3	*S*-site
Tyr179	**Tyr177**	**Phe222**	E2	Ether bridge
Leu199	Leu197	Met242	H5	Non-specific
Thr202	**Ile200**	**Thr245**	H5	*S*-site
Val203	**Ile201**	**Ile246**	H5	*S*-site
Leu207	Leu205	Leu249	H5	*S*-site
Trp378	Trp400	Trp504	H6	*R*-site
Tyr381	Tyr403	Tyr507	H6	*R*-site
Tyr404	Tyr426	Tyr529	H7	Piperidyl ring
Cys407	Cys429	Cys533	H7	Piperidyl ring
Tyr408	Tyr430	Tyr534	H7	*N*-Methyl

[a] H, helix; E, extracellular loop.

In the case of (*R*)-configured benzilates, the substituted ring is located in the hydrophobic *R*-site (Fig. 5, **B**). Possibilities of stabilizing hydrogen bridges are missing in the *R*-site which causes consequently a reduction of the affinity for (*R*)-benzilates. This more hydrophilic *S*-site of the M1 receptor was also found in the binding model for M2 and M3 receptor, which should result in an increased affinity for (*S*)-enantiomers. This assumption is supported by experimental binding data. A hydrophilic *S*-binding site was earlier predicted by the observed dependency of eudismic ratio with respect to hydrophobic/hydrophilic substituted benzilic derivatives (Fig. 2).

2.2.2. Affinity distinctions to muscarinic receptor subtypes. Diverse affinities to receptor subtypes (M1 $\geqslant$ M3 > M2) are most likely caused by amino acids which are not conserved within M1, M2 and M3 (Table 3). The exchange of Val203 (M1) by Ile246 (M3) contributes to the lower affinity at M3 compared to M1 (M1 $\geqslant$ M3). The substitution of Tyr179 (M1) by Phe222 (M3) is probably of more importance for diminished affinity as hydrogen bridges between the hydroxyl group of tyrosine and both the ether oxygen and the hydroxyl group of the ligand disappear. Alternatively, a new intramolecular hydrogen bridge of the ligand is built whereby this effect is slightly compensated. Although the M2 receptor disposes off a tyrosine, the affinity of M2 is lower compared to that of M3 (M2 < M3). Primarily, this is caused by non-conserved amino acids of the *S*-site. Strong hydrophilic interactions of M3 (as with M1) disappear by substitution of Thr245 (M3) through a relatively large hydrophobic side chain of Ile200 (M2). In addition, the binding pocket becomes narrower and the remaining interactions are adversely affected. This explains the reduction of affinities at M2 not only for (*S*)-enantiomers but also for (*R*)-enantiomers compared to M1 and M3.

Based on the findings of the receptor model more M3 selective compounds may be obtained by avoiding hydrogen bridging between the hydroxyl group of the ligand and Tyr179 (M1) simply by replacing the hydroxyl group with a hydrogen or alkyl substituent. 4-DAMP, a benzilic analogue without a hydroxyl group but with M3 selective properties (Table 3, Fig. 1), seems to enforce this assumption. Alternatively, a long-chained alkyl substituent, which is capable of interacting with the extracellular loops, may also improve M3 selectivity.

2.2.3. Effect of aromatic substituents. According to the receptor model it is clearly understood why hydrophilic substituents are more tolerated by all receptor subtypes instead of hydrophobic ones. The order of affinity within the hydrophilic substituents (dimethylamino– > trifluormethoxy– > methylsulfonyl–) at M1 receptor may be due to different partial charges of the aromatic substituents and consequently varying electrostatic attractions. Furthermore, these non-bonding interactions are modified by steric effects of the substituents.

2.2.4. Unsubstituted benzilates. The achiral unsubstituted *N*-methyl-4-piperidyl benzilate shows the highest experimental affinity to muscarinic receptors. Presumably,

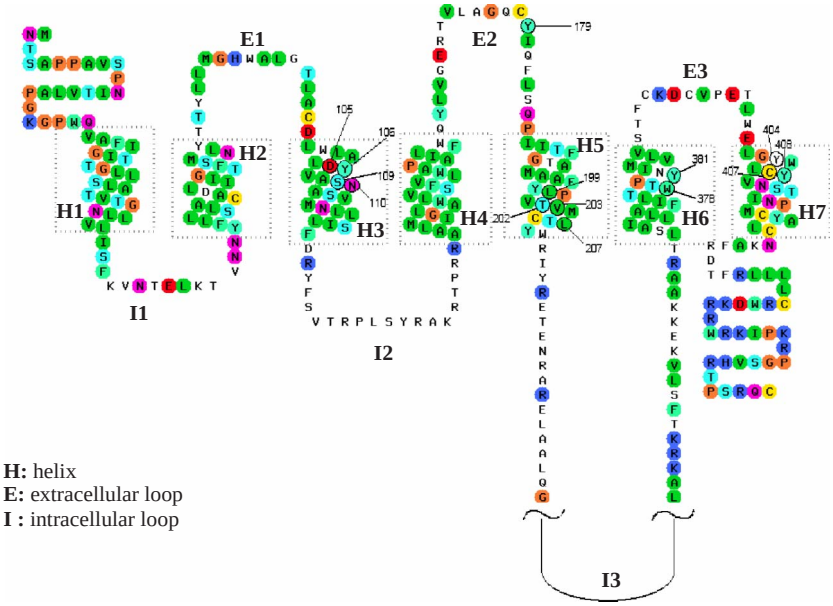

Figure 4. Snake-like presentation of M1 receptor with relevant amino acids (modified according to Ref. 19).

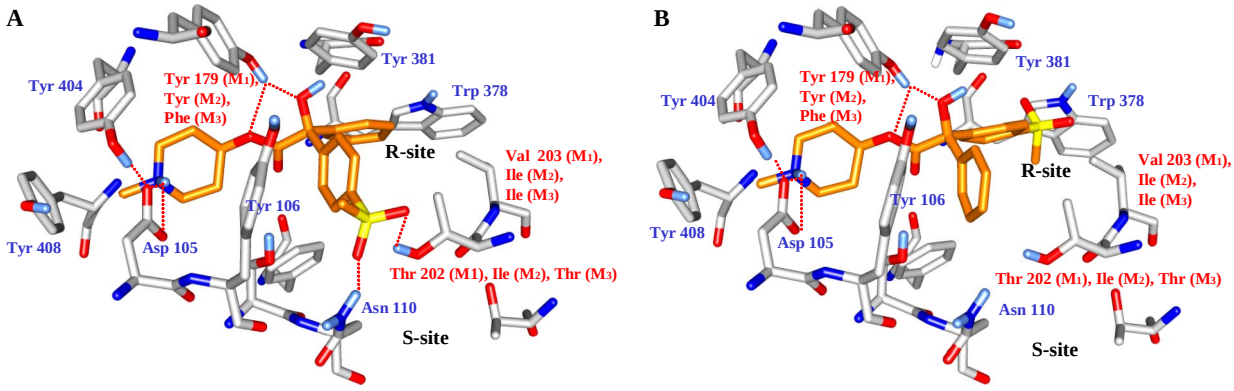

Figure 5. Binding of (*S*)-*N*-methyl-4-piperidyl 4-methylsulfonylbenzilate (**8**) **A** and (*R*)-*N*-methyl-4-piperidyl 4-methylsulfonylbenzilate (**7**) **B** at M1 receptor. Red labelled amino acids, non-conserved amino acids within the receptor subtypes M1, M2 and M3; red dotted lines, hydrogen bridges.

steric hindrance by aromatic substituents of the benzilates in the *S*- and *R*-binding site is entirely avoided. In that case, optimal hydrogen bonds between Asn110 and Thr202 can be formed since these residues are not interacting with substituents of the ligand.

2.2.5. Pharmacophoric conformation. There are two basic conformations of benzilic esters which occur preferentially. These are stabilized by an intramolecular hydrogen bridge between an ester function and a hydroxyl group (Fig. 6). On the one hand, there is a possible interaction between carbonyl oxygen (ester function) and the hydroxyl group (conformation A), on the other hand there is an interaction between the ether oxygen (ester function) and the hydroxyl group (conformation B). Both described conformations (A and B) were also found in X-ray crystal structures of benzilic derivatives.[20]

Interestingly, the performed molecular modelling studies revealed conformation B as a pharmacophoric conformation (Fig. 5). Investigations of rigid analogues done by Flavin et al., in which the hydrogen bridge was replaced by a covalent bond[13], support the calculated conformation B.

2.2.6. Quantitative evaluation of the receptor ligand complex. The interaction energies (IE) of all optimized receptor ligand complexes were calculated by subtracting the energies of the most stable conformations of the isolated ligands (E_L) and of the empty receptor

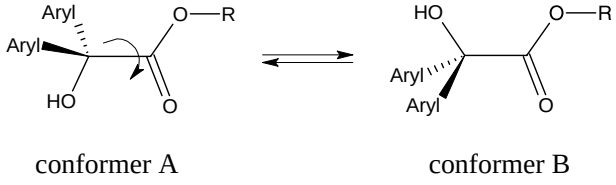

Figure 6. Preferred conformations of benzilic esters.

Table 4. Interaction energies of benzilic derivatives

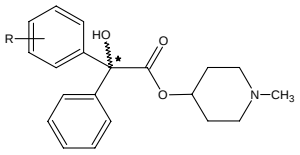

Substitution R		pK_i [a]	E_{RL} (kcal/mol)	E_R (kcal/mol)	E_L (kcal/mol)	IE (kcal/mol)	Receptor subtype
4-CH_3–SO_2–	*S*	8.37	−2214.5	−2160.5	22.1	−76.1	M1
	R	6.58	−2200.5	−2160.5	22.1	−62.1	M1
4-F_3CO–	*S*	8.91	−2220.4	−2160.5	23.9	−83.8	M1
	R	7.39	−2211	−2160.5	23.9	−74.4	M1
4-*tert*-C_4H_9–	*S*	8.29	−2221.7	−2160.5	23.9	−85.1	M1
	R	7.52	−2203.1	−2160.5	23.9	−66.5	M1
4-$(CH_3)_2N$–	*S*	8.98	−2209.9	−2160.5	43.9	−93.3	M1
	R	7.34	−2181.2	−2160.5	43.9	−64.6	M1
H	—	9.94	−2230.8	−2160.5	22.6	−92.9	M1
Dioxolo-[b]	—	8.45	−2187.4	−2160.5	50.6	−77.5	M1
4.4′-Bis(F_3CO–)	—	8.77	−2219.1	−2160.5	22.9	−81.5	M1
4-CH_3–SO_2–	*S*	7.15	−2212.6	−2166.4	22.1	−68.3	M2
	R	5.80	−2191.6	−2166.4	22.1	−47.3	M2
4-F_3CO–	*S*	8.61	−2226.8	−2166.4	23.9	−84.3	M2
	R	6.84	−2209.4	−2166.4	23.9	−66.9	M2
4-*tert*-C_4H_9–	*S*	7.48	−2219.2	−2166.4	23.9	−76.7	M2
	R	6.69	−2207.1	−2166.4	23.9	−64.6	M2
4-$(CH_3)_2N$–	*S*	7.28	−2195.2	−2166.4	43.9	−72.7	M2
	R	6.73	−2188.6	−2166.4	43.9	−66.1	M2
Dioxolo-[b]	—	8.18	−2198.8	−2166.4	50.6	−83.0	M2
4-CH_3–SO_2–	*S*	7.77	−2221.7	−2169.6	22.1	−74.2	M3
	R	6.39	−2204.6	−2169.6	22.1	−57.1	M3
4-F_3CO–	*S*	8.40	−2224.4	−2169.6	23.9	−78.7	M3
	R	7.08	−2211.4	−2169.6	23.9	−65.7	M3
4-*tert*-C_4H_9–	*S*	7.84	−2216.8	−2169.6	23.9	−71.1	M3
	R	7.52	−2211.3	−2169.6	23.9	−65.6	M3
4-$(CH_3)_2N$–	*S*	7.46	−2199.6	−2169.6	43.9	−73.9	M3
	R	7.08	−2189.3	−2169.6	43.9	−63.6	M3
Dioxolo-[b]	—	8.22	−2192.6	−2169.6	50.6	−73.6	M3
4.4′-Bis(F_3CO–)	—	8.24	−2225.6	−2169.6	22.9	−78.9	M3

[a] Experimentally determined pK_i values.

[b]

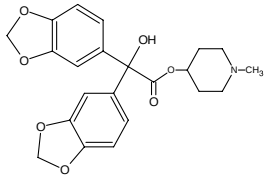

(E_R) from the receptor ligand complex (E_{RL}) with the lowest energy (Table 4).[21]

$$IE = E_{RL} - (E_R + E_L).$$

A correlation between interaction energies and experimental binding constants can be assumed because all structures have similar entropy contribution (number of rotating bonds) and solvation energies. According to the Gibbs–Helmholtz equation, interaction energy and binding constant should have a linear correlation. An attempt to predict the binding affinity by using SCORE[22] failed. The calculated pK_d values show only rudimentary correlation to the experimental binding data.

As the interaction energy becomes more negative, the receptor ligand complex becomes stronger. This results in an increased binding affinity. Overall, thirty interaction energy values at M1, M2 and M3 were calculated and put in relation to their respective experimental binding data. The obtained squared correlation coefficient, $R^2 = 0{,}857$, emphasizes the quality of the receptor ligand binding model for benzilates (Fig. 7).

3. Conclusions

Structural parameters such as absolute configuration and aromatic substitution of chiral *N*-methyl-4-piperidyl

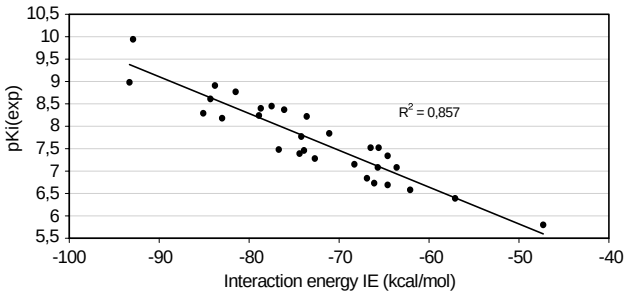

Figure 7. Correlation of experimental pK_i values with calculated interaction energies of benzilic derivatives with the M1/M2/M3 receptors.

benzilates were modified and their effect on affinity and subtype selectivity was investigated. The absolute configuration appears to have the largest effect with the (*S*)-configuration always superior in affinity up to 61-fold at the M1 receptor. A further increase in affinity is achieved by hydrophilic substitution. *N*-Dimethylamino substituent exhibits the best binding results of all derivatives tested. Additionally, absolute configuration, aromatic substitution and alcoholic ester components have an impact on the affinity ratio towards receptors M1/M2/M3. (*S*)-Configuration promotes M1-binding compared to M3, and (*R*)-configuration intensifies M3-binding although M1 affinity always dominates. Thus, the (*S*)-enantiomer of the *N*-dimethylamino derivative stands out as M1 selective compound (M1/M2 23-fold, M1/M3 61-fold).

Models of the receptor ligand complex were developed with the aid of molecular modelling techniques. The diverse affinities and selectivities at muscarinic receptors of enantiomeric benzilate are comprehensively explained by the generated models. In prospective work, further structural optimization of benzilic derivatives may be achieved based on these receptor models. (*S*)-configured benzilates should serve as lead structures for M1 selective compounds, whereas (*R*)-configured benzilates could serve as lead structures for M3 selective compounds.

4. Experimental

4.1. Radioligand binding studies

The assays were conducted by Mrs. Waelbroeck (Faculte de Médecine, Laboratoire de Chimie Biologique et de la Nutrition, Brussels) using CHO cell lines, transfected, respectively, with plasmids encoding hM1, hM2 and hM3. [^{3}H]-*N*-methylscopolamine ([^{3}H]NMS) was applied as radioligand. The non-specific binding was defined as binding in the presence of 10 μM atropine. The radioactivity was counted in a Packard 1500 Tricarb liquid scintillation analyser.

4.1.1. Data analysis. Each competition curve was repeated three times in duplicate. The experimental data were analysed by non-linear curve fitting, using the GRAPHPAD Software.[23] The unlabelled drugs K_i values were calculated, assuming that they competitively inhibited [^{3}H]NMS binding, using the Cheng and Prusoff equation. The pK_i and standard errors of the determination are summarized in Table 2. The hill coefficients of all competition curves were 1. In the experiments presented herein, the [^{3}H]NMS K_D values were 0.27 nM (M1), 0.46 nM (M2) and 0.27 nM (M3).

4.2. Molecular modelling

4.2.1. Modelling of the muscarinic receptors (M1, M2 and M3). Based on the X-ray structure of bovine rhodopsin (PDB access 1F88), all three muscarinic receptors have been modelled using the tools of modelling program MOE.[24] The muscarinic receptors posses an extraordinarily long intracellular third loop. The sequences 218 to 358 (M1), 218 to 381 (M2) and 261 to 484 (M3) of the muscarinic receptors were removed in order to allow appropriate alignment with the sequence of the X-ray structure of bovine rhodopsin. Since the considered binding site is located in the seven transmembrane region, this sequence deletion will not influence the docking studies of the ligands. The alignment of the whole sequences with the template showed an identity score of 40% on average, but for seven transmembrane helices a homology of up to 60% which should guarantee homology modeling of the muscarinic receptors with reasonable quality. The sequences were aligned using the blosum 62-matrix (Henikoff and Henikoff, 1992, 1993). Ten gas-phase models have been calculated by MOE. Subsequently, the models were refined and energetically optimized using the amber94 force field (gradient below 0.05). All ten models were checked with regard to stereochemical quality using PROCHECK.[25] After manual correction of conformations of up to four single residues in the intracellular loops and reoptimization (gradient lower than 0.05), the backbone dihedral angle distribution of all amino residues (RAMACHANDRAN plot) showed 78% in most favoured, 18% in additional allowed and 4% in generously allowed regions and none in disallowed regions. All other stereochemical parameters were inside the quality expected for a structure with a resolution of 2.0 Å.

4.2.2. Docking studies. The model with the best quality (most residues in favoured areas) was used for docking studies. Twenty different docking arrangements for each ligand were created by means of the automatic docking program GOLD[26] with standard settings and GOLDScore as fitness function. One oxygen atom of conserved aspartic acid of transmembrane helix three was taken as target point for the docking calculations. Since GOLD considers the protein rigid during the docking of the ligands molecular dynamics simulations were performed to simulate an induced fit mechanism. All clearly different docking arrangements were taken as a start for a short molecular dynamics simulation (10 ps, 300 K) with subsequent energy optimization using the TRIPOS force field[27] and GASTEIGER charges.[28] During these calculations, the backbone atoms of the receptor were kept

fixed but the ligands and all side chain atoms were flexible. In all cases, the alterations of the side chain conformations during the dynamics simulations were very small due to the almost completely occupied space by the docked ligands. For each ligand, a systematic conformational search of all flexible dihedral angles was performed using MOE and the TRIPOS force field including GASTEIGER charges. The interaction energies of all ligands with the receptors were calculated by subtracting the energies of the most stable conformations of the isolated ligands and of the empty receptor from the ligand receptor complex with the lowest energy (Table 4).

References and notes

1. Ward, S. D. C.; Curtis, C. A. M.; Hulme, E. C. *Mol. Pharmacol.* **1999**, *56*, 1031–1041.
2. Allman, K.; Page, K. M.; Curtis, CA.; Hulme, E. C. *Mol. Pharmacol.* **2000**, *58*, 175–184.
3. Lu, Z. L.; Saldanha, J. W.; Hulme, E. C. *J. Biol. Chem.* **2001**, *276*, 34098–34104.
4. Adam, O.; Dörfler, H.; Forth, W. *Deutsches Ärztebaltt* **2001**, *98*, A840.
5. Battock, T. M.; Castelden, C. M. *Br. Med. Bull.* **1990**, 147–155.
6. Chapple, C. *Urology* **2000**, *55*, 33–46.
7. Eglen, R.; Watson, N. *Pharmacol. Toxicol.* **1996**, *78*, 59–68.
8. Bierwisch, M. Synthese und Charakterisierung neuer potentieller M3-selektiver Anticholinergika mit Diphenylessigsäurestruktur zur Therapie der Harninkontinenz, Dissertation; Humboldt-Universität zu Berlin, 2002.
9. Schwartz, T. Lecture: Structure-based drug discovery in 7TM receptors based on knowledge on molecular mechanism of activation. GDCh/DPhG Annual Meeting March 15–17, 2004 (Erlangen).
10. Vorwerk, Th.; Fröhlich, L.; Göber, B. *Pharmazie* **2001**, *56*, 595–609.
11. Vorwerk, Th. Untersuchungen zu Synthese, Analytik, Stabilität und Pharmakologie neuer substituierter Piperidylbenzilate (Dissertation); Humboldt-Universität zu Berlin, 2000.
12. Selent, J.; Pamperin, D.; Göber, B. Preparation, Characterization and Binding Properties of Chiral Substituted *N*-Methyl-4-piperidyl Benzilates, expected in 2006.
13. Flavin, M. T.; Lu, M. C.; Thompson, E. B.; Bhargava, H. N. *J. Med. Chem.* **1987**, *30*, 278–285.
14. Recanatini, M.; Tumiatti, V.; Budriesi, R.; Chiarini, A.; Sabatino, P.; Bolognesi, M. L.; Melchiorre, C. *Bioorg. Med. Chem.* **1995**, *3*, 267–277.
15. Hulme, E. C.; Lu, Z. L. *Biochem. Soc. Trans.* **2003**, *31*, 29–34.
16. Hulme, E. C.; Lu, Z. L. *Receptor Channel* **2003**, *9*, 215–228.
17. Hulme, E. C.; Curtis, C. A. M. *Life Sci.* **1995**, *56*, 891–898.
18. Kiesewetter, D. O.; Silverton, J. V.; Eckelman, W. C. *J. Med. Chem.* **1995**, *38*, 1711–1719.
19. Campagne, F.; Maigret, B. (Laboratoire de Chimie Théorique de Nancy, U.A. CNRS 510, B.P. 239 - 54506 Vandoeuvre-les-Nancy CEDEX, France) and Bernassau, J., M. (Sanofi Recherche, 371, Rue du Pr. Blayac, 34184 Montpellier CEDEX 4, France): Snake-like Diagram of M1-Receptor.
20. Selent, J. Darstellung und Charakterisierung neuartiger,chiraler, basischer Benzilsäureester mit anticholinerger Wirkung (Dissertation), Humboldt-Universität zu Berlin, 2004.
21. Höltje, H.-D.; Folkers, G. Molecular Modeling; Band 5, Weinheim, VCH, 1997.
22. Wang, R.; Liang, L. *J. Mol. Model.* **1998**, *4*, 379–394.
23. GRAPHPAD Software, 11452 El Camino Real, #215, San Diego, CA 92130 USA.
24. MOE (Molecular operating environment), Chemical Computing Group, Montreal, Canada.
25. Laskowski, R. A.; MacArthur, M. W.; Moss, D. S.; Thornton, J. M. *J. Appl. Crystallogr.* **1993**, *26*, 283–291.
26. GOLD-Copyright-Cambridge Crystallographic DataCentre-1998-located in Cambridge, UK.
27. Clark, M.; Cramer, R. D., III; van Opdenbosch, N. J. *J. Comput. Chem.* **1989**, *10*, 982–1012.
28. Gasteiger, J.; Marsili, M. *Tetrahedron* **1980**, *36*, 3219–3228.